Preparation of tungsten oxide nanowires from sputter-deposited WC_x films using an annealing/oxidation process

Shui-Jinn Wang,[a] Chao-Hsuing Chen, Rong-Ming Ko, Yi-Cheng Kuo, Chin-Hong Wong, and Chien-Hung Wu
Institute of Microelectronics, Department of Electrical Engineering, National Cheng Kung University, Tainan, Taiwan, Republic of China

Kai-Ming Uang, Tron-Min Chen, and Bor-Wen Liou
Department of Electrical Engineering, Wu-Feng Institute of Technology, Chiayi 62153, Taiwan, Republic of China

(Received 8 March 2005; accepted 26 May 2005; published online 20 June 2005)

The self-synthesis of tungsten oxide ($W_{18}O_{49}$) nanowires on sputter-deposited WC_x films using a simple annealing/oxidization process was reported. It was found that thermal annealing of WC_x films at 680 °C for 30 min in nitrogen followed by oxidation at 450 °C for 30 min in pure oxygen would yield dense and well-crystallized monoclinic $W_{18}O_{49}$ (010) nanowires with a typical length/diameter of about 0.15–0.2 μm/10–20 nm. The formation of $W_{18}O_{49}$ nanowires is attributed to the nuclei of immature W_2C nanowires experiencing a regrowth process, accompanied by carbon depletion and the oxidization of tungsten during the subsequent oxidization process. © *2005 American Institute of Physics*. [DOI: 10.1063/1.1957115]

Transition metal oxides are a large family of materials exhibiting various distinctive electrochromic, optochromic, and gaschromic properties.[1–4] For device applications, such as flat panel display, optical modulation devices, auto dimming mirror, gas sensors, humidity, and temperature sensors etc.,[1–7] nanoscaled tungsten oxides (WO_x) are attractive because they exhibit physical and chemical properties that are very different from their bulk counterparts. Essentially, the sensitivity and response of WO_x-related sensors could be substantially improved and the working temperature could also be reduced due to the larger surface area, enormous number of surface atoms, and/or dimensional confinement of electrons.[7] It is interesting and important from a technological point of view concerning the development of simple and effective ways for preparing tungsten oxide nanoparticles.[1,7] Nonetheless, studies on nanoscaled WO_x materials are still limited for the past decade due to the lack of an appropriate preparation method. Recently, the preparation of WO_x nanowires has been reported by many research groups.[8–10] However, these methods are either technically complex,[9] not compatible with complementary metal-oxide-semiconductor technology,[8] or incapable of pattern growth.[10] Therefore, efforts to develop a simple method for the synthesis of WO_x nanowires for device applications without the above-mentioned drawbacks are still required.

In this work, a thermal annealing/oxidization process was employed to synthesize tungsten oxide ($W_{18}O_{49}$) nanowires on sputter-deposited WC_x films. Thermal annealing of WC_x films was carried out in a nitrogen ambient with a deficient thermal budget to grow W_2C nanowires self-catalytically. These immature nanowires were then served as precursors or nuclei for the growth of tungsten oxide nanowires in a subsequent oxidization process. The oxidation conditions and suitable thermal budget for the formation of well-crystallized tungsten oxide nanowires were investigated. The possible mechanism behind the regrowth and conversion of nanowires was also proposed.

In experiments, 4 in. *n*-type Si(100) wafers with a resistivity of 1–10 Ω cm were used as the substrate. The WC_x target used for the deposition of WC_x films was 50:50 (wt %) in composition and 99.5% in purity. After a presputtering procedure of WC_x target with a power of 60 W for 10 min, the WC_x films were deposited at a power of 200 W in an argon ambient with a flow rate of 24 sccm without substrate biasing or heating. During sputtering, the base and sputtering pressure were kept at 2×10^{-6} and 7.6×10^{-3} Torr, respectively. The thickness of WC_x films was 60 nm and the deposition rate was about 0.4 Å/s. Since the growth of well-crystallized tungsten oxide nanowires is very difficult from the direct oxidation of sputter-deposited WC_x films, here a simple thermal annealing/oxidization process was proposed to grow α-W_2C nanowires self-catalytically first, and then convert them into tungsten oxide nanowires.

To prepare W_2C nanowires, the WC_x films were subjected to a quartz furnace to synthesize α-W_2C nanowires at 680 °C for 30 min in N_2 ambient.[11] Because the thermal budget arising from all thermal processing steps plays a crucial role in the final status of the grown nanowires,[12] the thermal annealing temperature was reduced intentionally from the optimum value of 700 °C to 680 °C to cover the thermal budget coming from subsequent oxidization.[11] It is noted that the pattern growth of W_2C nanowires can be easily achieved by defining the deposited WC_x films photolithographically before the thermal annealing process. After that, the annealed samples were oxidized in O_2 ambient at 300–500 °C for 30 min to have the immature W_2C nanowires regrown and transformed into tungsten oxide nanowires.

Figure 1 shows the scanning electron microscopy (SEM) image of the surface morphology of WC_x films before and after oxidation at 450° C in an O_2 ambient for 30 min. Since the synthesized temperature was intentionally reduced, the W_2C nanowires shown in the inset were not fully developed

[a]Electronic mail: sjwang@mail.ncku.edu.tw

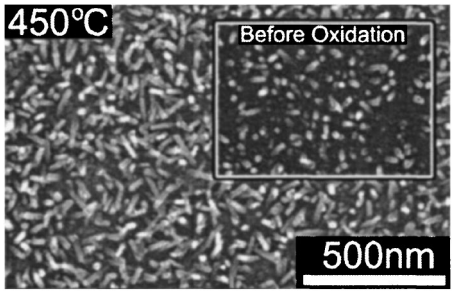

FIG. 1. The SEM image of the 680 °C-annealed sample after oxidation at 450 °C for 30 min in an O_2 ambient. Inset is the image of the 680 °C-annealed sample before oxidation.

yet. It is found that the phase change from WC_x to W_2C caused by the decarburization of WC_x films during thermal annealing is responsible for the self-catalytic growth of W_2C nanowires.[11] After oxidization, it is seen that the surface of the sample turns from silver to reddish violet in color, and both the length and density of nanowires apparently increase. The length/diameter of the oxidized nanowires shown in Fig. 1 was in the range of 0.15–0.2 μm/10–20 nm. Densities of nanowires estimated from SEM images of the 300, 350, 400, 450, and 500 °C-oxidized samples were about 165, 145, 130, 330, and 180 μm^{-2}, respectively. Note that the 450 °C-oxidized sample has the highest density of nanowires. The same situations were also observed for WC_x films with other thickness ranging from 15–60 nm.

Figure 2 presents the transmission electron microscopy (TEM) image and selected-area electron diffraction (SAED) pattern of nanowire obtained from the 450 °C-oxidized samples. The length and diameter of the wire shown in the low-left inset of Fig. 2 is about 0.2 μm and 10 nm, respectively. Clear stripes of lattice plane and the associated SAED pattern indicate that the nanowire is well crystallized. The inter plane distance of *d* space was determined to be 3.78 Å. The crystallization phase of the wire could be identified as nonstoichiometric monoclinic $W_{18}O_{49}$ (010) according to JCPDS Card no. 36-0101. Since $W_{18}O_{49}$ has a close-packed plane of (010), nanowires prepared by the present work thus grow along the [010] direction. The crystallization phase of $W_{18}O_{49}$ (010) is similar to that prepared by chemical vapor deposition[9] or synthesized on tungsten plates.[8]

The typical x-ray diffraction (XRD) patterns of the annealed samples before and after oxidation at different temperatures are shown in Fig. 3. Note that the broad peak at

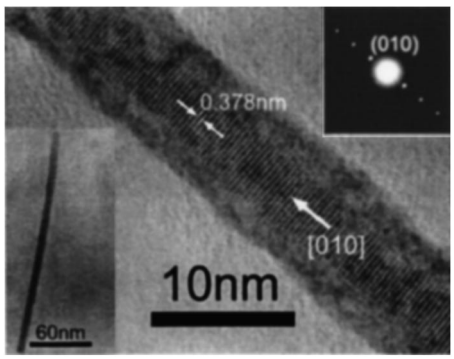

FIG. 2. TEM images of the $W_{18}O_{49}$ nanowire obtained from sputter-deposited WC_x films after thermal annealing (at 680 °C for 30 min) and oxidization (at 450 °C for 30 min). Inset is the SAED pattern for a single $W_{18}O_{49}$ nanowire.

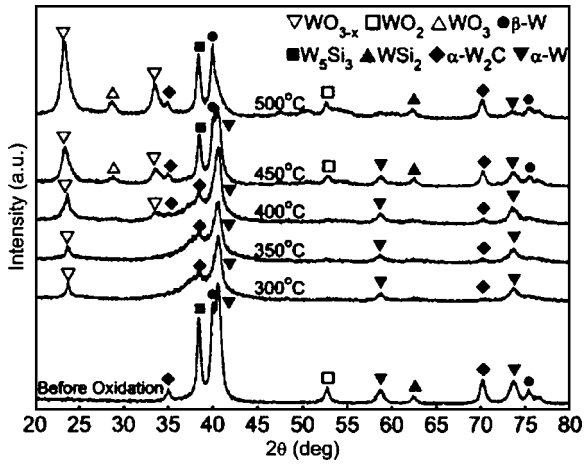

FIG. 3. XRD patterns of 680 °C-annealed samples with and without oxidization. Oxidization was performed at 300–500 °C in O_2 for 30 min.

around 38.03° is an indication of α-W_2C (002) nanowires, while the sharp peak at around 38.3° corresponds to the bulk W_5Si_3 phase.[11] Comparing the samples of before and after oxidization, it is observed that the oxidization at 300, 350, and 400 °C had caused the regrowth of W_2C nanowires and the oxidization of nanowires as revealed by the main peak at around 23°–24° corresponding to WO_2, WO_3, and nonstoichiometric WO_{3-x}. However, as the oxidization temperature was increased to 450 or 500 °C, the peak at around 38° became sharp and peak intensity of around 23°–24° was more intensive, indicating that the conversion from W_2C nanowires to tungsten oxide nanowires was significantly increased. Note that the peak at around 23°–24° was seen slightly shifting from 23.76° for 300 °C-oxidized samples to 23.4° for 500 °C-oxidized samples.

To further explore the possible phase transitions that occurred in oxidized samples, the spectra ranging from 23° to 24° were smoothened and deconvoluted into several Gaussian peaks as shown in Fig. 4. Here, peaks corresponding to the nonstoichiometric monoclinic, orthorhombic, triclinic, tetragonal, and cubic WO_x ($2.72 \leqslant x \leqslant 3$) crystallites were de-

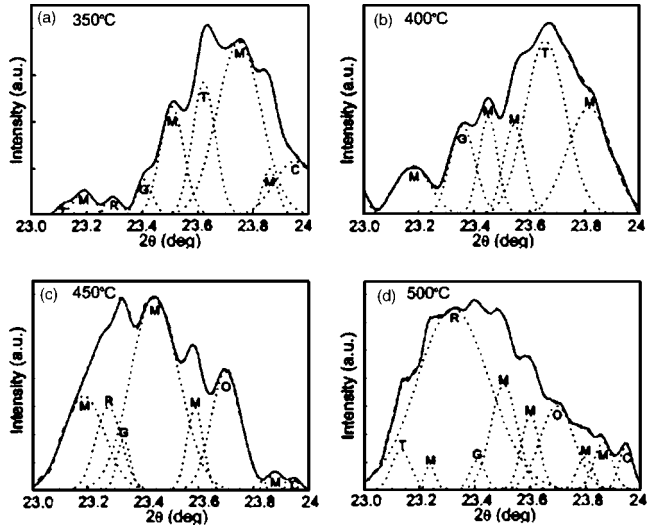

FIG. 4. XRD spectra of 350–500 °C oxidized samples in the range of 23°–24°. The anomalous peaks have been deconvoluted into several Gaussian peaks corresponding to monoclinic (M), orthorhombic (O), triclinic (T), tetragonal (G), and cubic (C) of WO_x crystallites, and the orthorhombic WO_2 (R).

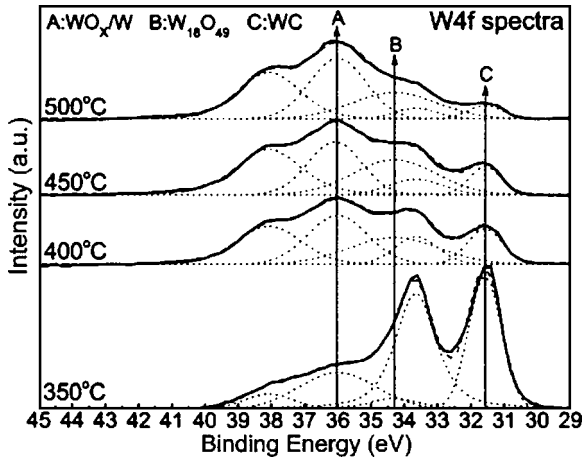

FIG. 5. The surface XPS W 4*f* spectra of 680 °C-annealed samples after oxidization at 350–500 °C.

noted by M, O, T, G, and C, respectively, while the peak corresponding to the orthorhombic WO_2 was denoted by R. As is evident in Fig. 4, the strongest peak for the 350, 400, 450, and 500 °C-oxidized samples was monoclinic $W_{18}O_{49}$ (103) (~23.75°), triclinic WO_3 (020) (~23.65°), monoclinic $W_{18}O_{49}$ (010) (~23.45°), and orthorhombic WO_2 (111) (~23.32°), respectively. Note that the strongest peak position for the 450 °C-oxidized samples falls in the region of monoclinic $W_{18}O_{49}$ (010). Accordingly, the M peak at 23.45°–23.5° would be a good indicator for the appearance of well-crystallized monoclinic $W_{18}O_{49}$ (010) nanowires. Based on the SEM images and XRD analysis mentioned above, it can be concluded that the oxidation temperature of 450 °C would yield the densest and purest monoclinic $W_{18}O_{49}$ (010) nanowires.

To investigate the possible mechanism governing the regrowth and conversion of nanowires, chemical bonding states of the oxidized samples were characterized by x-ray photoelectron spectroscopy (XPS) as shown in Fig. 5. Note that the O 1*s* spectra of 350–500 °C samples all have similar peaks at around 530.8–531 eV (not shown) which indicate the existence of WO_2 and WO_3 crystalline phases.[13,14] In Fig. 5, the W 4*f* spectra can be deconvoluted into five Gaussian peaks, which were at ~31.58 (W $4f_{7/2}$ of WC, denoted as Peak C), ~33.65 (W$4f_{5/2}$ of WC), ~34.3 (W $4f_{7/2}$ of $W_{18}O_{49}$, denoted as Peak B), ~36 (W $4f_{7/2}$ of WO_x/W, denoted as Peak A), and ~38.07 eV (W $4f_{5/2}$ of WO_x/W), respectively.[15–17] Note that the intensity of Peaks A and B increases with increasing the oxidization temperature, while Peak C has an inverse situation. It could be ascribed to the fact that the degree of carbon depletion and chemical reaction between W and O increases with the oxidization temperature, which should be responsible for the mechanism governing the conversion of W_2C to $W_{18}O_{49}$ nanowires. Note that Peak B of 450 °C-oxidized samples has the highest intensity, indicating that it should have the densest $W_{18}O_{49}$ nanowires, which is in good agreement with both the SEM images and XRD analysis.

In summary, W_2C nanowires self-synthesized from sputter-deposited WC_x films by thermal annealing in N_2 ambient have been used as precursors or nuclei for the formation of tungsten oxide nanowires. The conversion of W_2C nanowires to $W_{18}O_{49}$ ones is attributed to carbon depletion accompanying with the chemical reaction of W and O inside nanowires during oxidation process. According to material analysis, tungsten oxide nanowires are well crystallized and mainly comprised of nonstoichiometric monoclinic $W_{18}O_{49}$ (010). The length, diameter, and density of $W_{18}O_{49}$ nanowires obtained from the 450 °C-oxidized sample are of 0.15–0.2 μm, 10–20 nm, and 330–340 μm^{-2}, respectively. It has been found that annealing condition of 680 °C/30 min for growing W_2C nanowires as the precursors, and 450 °C/30 min for synthesizing $W_{18}O_{49}$ nanowires would yield tungsten oxide nanowires with the highest density and purity.

This work was supported by the National Science Council (NSC) of Taiwan, Republic of China, under Contract No. NSC 93-2215-E-006-001. Technical assistance from the Center for Micro/Nano Technology Research, National Cheng Kung University, Tainan, Taiwan, is appreciated.

[1] Y. Koltypin, S. I. Nikitenko, and A. Gedanken, J. Mater. Chem. **12**, 1107 (2002).
[2] C. Santato, M. Odziemkowski, M. Ulmann, and J. Augustynski, J. Am. Chem. Soc. **123**, 10639 (2001).
[3] C. Sella, M. Maaza, O. Nemraoui, J. Lafait, N. Renard, and Y. Sampeur, Surf. Coat. Technol. **98**, 1477 (1998).
[4] Y. Zhao, Z. C. Feng, and Y. Liang, Sens. Actuators B **66**, 171 (2000).
[5] H. Meixner, J. Gerblinger, U. Lampe, and M. Fleischer, Sens. Actuators B **23**, 119 (1995).
[6] J. L. Solis, S. Saukko, L. Kish, C. G. Granqvist, and V. Lantto, Thin Solid Films **391**, 255 (2001).
[7] L. G. Teoh, I. M. Hung, J. Shieh, W. H. Lai, and M. H. Hon, Electrochem. Solid-State Lett. **6**, G108 (2003).
[8] G. Gu, B. Zheng, W. Q. Han, S. Roth, and J. Liu, Nano Lett. **2**, 849 (2002).
[9] X. L. Li, J. F. Liu, and Y. D. Li, Inorg. Chem. **42**, 921 (2003).
[10] J. Liu, Y. Zhao, and Z. Zhang, J. Phys.: Condens. Matter **15**, L453 (2003).
[11] S. J. Wang, C. H. Chen, S. C. Chang, K. M. Uang, C. P. Juan, and H. C. Cheng, Appl. Phys. Lett. **85**, 2358 (2004).
[12] S. J. Wang, C. H. Chen, S. C. Chang, C. H. Wong, K. M. Uang, T. M. Chen, R. M. Ko, and B. W. Liou, Nanotechnology **16**, 273 (2005).
[13] F. P. J. Kerkhof, J. A. Moulijn, and A. Heeres, J. Electron Spectrosc. Relat. Phenom. **14**, 453 (1978).
[14] D. D. Sarma and C. N. R. Rao, J. Electron Spectrosc. Relat. Phenom. **20**, 25 (1980).
[15] R. J. Colton and J. W. Rabalais, Inorg. Chem. **15**, 237 (1976).
[16] P. Biloen and G. T. Pott, J. Catal. **30**, 169 (1973).
[17] I. Kojima and M. Kurahashi, J. Electron Spectrosc. Relat. Phenom. **42**, 177 (1987).